

(Fig. 4). This strategy could be generalized to the simultaneous analysis of several loci. For each set of two labeled, allele-specific oligonucleotides and one unlabeled, the latter is given a nonhybridizing 3' sequence extension of a unique length. This results in different migration rates for the ligation products, characteristic of each locus.

In contrast to gene detection techniques based on immobilizing the target DNA, such as DNA blots, the hybridization reported here was performed in solution and in a small volume, which reduced the time required for hybridization (17). It also obviated the step of immobilizing the target DNA. Both ligation and binding of the biotinylated oligonucleotides are efficient and rapid steps that should permit quantitative detection of target molecules. In general, there are three rate-limiting steps in gene detection techniques. The first is sample preparation, which can be greatly simplified as demonstrated here. The second is the time required for the probes to anneal to the target sequence. This is a function of the concentration of the probe and can be reduced considerably. The third and most time-consuming step in the present technique is signal detection by autoradiography. A sufficiently sensitive fluorescent detection method (18) should drastically reduce this time, permitting the development of a rapid, automated gene detection procedure.

REFERENCES AND NOTES

- C. T. Caskey, *Science* **236**, 1223 (1987).
- A. Svejgaard *et al.*, *Immunol. Rev.* **70**, 193 (1983); J. L. Tiwari and P. I. Terasaki, *HLA and Disease Associations* (Springer-Verlag, New York, 1985).
- V. A. McKusick, *Mendelian Inheritance in Man* (Johns Hopkins Univ. Press, Baltimore, ed. 7, 1986).
- D. N. Cooper and J. Schmidtke, *Lancet* **i**, 273 (1987).
- J. I. Rotter and J. M. Diamond, *Nature* **329**, 289 (1987).
- B. J. Conner *et al.*, *Proc. Natl. Acad. Sci. U.S.A.* **80**, 278 (1983); N. M. Whiteley, M. W. Hunkapiller, A. N. Glazer, European Patent application 0 185 494 A2 (1986).
- R. M. Myers *et al.*, *Nature* **313**, 495 (1985).
- R. F. Geever *et al.*, *Proc. Natl. Acad. Sci. U.S.A.* **78**, 5081 (1987).
- R. M. Myers, Z. Larin, T. Maniatis, *Science* **230**, 1242 (1985); E. Winter, F. Yamamoto, C. Almo-guera, M. Perucho, *Proc. Natl. Acad. Sci. U.S.A.* **82**, 7575 (1985).
- T. Hunkapiller, personal communication.
- R. K. Saiki, T. L. Bugawan, G. T. Horn, K. B. Mullis, H. A. Erlich, *Nature* **324**, 163 (1986).
- R. M. Winslow and W. F. Anderson, in *The Metabolic Basis of Inheritance*, J. B. Stanbury, J. B. Wyngaarden, D. S. Fredrickson, J. L. Goldstein, M. S. Brown, Eds. (McGraw-Hill, New York, 1983), pp. 1666-1710.
- J. A. Kark, D. M. Posey, H. R. Schumacher, C. J. Ruehle, *N. Engl. J. Med.* **317**, 781 (1987).
- R. K. Saiki *et al.*, *Science* **230**, 1350 (1985).
- R. K. Saiki, N. Arnheim, H. A. Erlich, *Biotechnology* **3**, 1008 (1985).
- L. M. Smith *et al.*, *Nature* **321**, 674 (1986); C. Connell *et al.*, *BioTechniques* **5**, 342 (1987).
- J. G. Wetmur and N. Davidson, *Mol. Biol.* **31**, 349 (1968).
- E. Soini and H. Kojola, *Clin. Chem.* **29**, 65 (1983).
- Genomic DNA was purified from guanidinium HCl-solubilized cells as described [D. Bowtell, *Anal. Biochem.* **162**, 463 (1987)] and resuspended by boiling before adding 7 μ g in 4 μ l of water per assay well. The plasmid and genomic DNA samples were denatured by adding 1 μ l of 0.5M NaOH and incubating for 10 min at 37°C before restoring the pH with 1 μ l of 0.5M HCl. Alternatively, samples of nucleated blood cells were used directly as a source of DNA for the analysis. Cells (10^6), obtained by Ficoll-Hypaque (Pharmacia) flotation, were added in 50 μ l of phosphate-buffered saline to each well.
- The oligonucleotides were assembled by the phosphoramidite method [S. J. Horvath, J. R. Firca, T. Hunkapiller, M. W. Hunkapiller, L. Hood, *Methods Enzymol.* **154**, 314 (1987)] on an Applied Biosystems model 380A DNA synthesizer and purified either by polyacrylamide gel electrophoresis or reversed-phase high-pressure liquid chromatography (HPLC). Biotinylation was performed by reacting a biotin *N*-hydroxysuccinimide ester (Enzotin, Enzo) with a 5' aminothymidine residue incorporated in the oligonucleotide [L. M. Smith, S. Fung, T. J. Hunkapiller, M. W. Hunkapiller, L. Hood, *Nucleic Acids Res.* **13**, 2399 (1985)]. The product was purified by reversed-phase HPLC.
- The size of the area on which the beads were deposited was reduced by interposing a 3-mm-thick plexiglass disk with conical holes with diameters of 5 mm on the upper surface and 2 mm on the lower.
- The authors acknowledge a stipend from the Knut and Alice Wallenberg Foundation to U.L. and support from NSF grant BNS 87 14486, Defense Advanced Research Projects Agency grant N00014-86K-0755, Upjohn Company, and Applied Biosystems, Inc. The oligonucleotides were synthesized by S. J. Horvath and the fluorescence data were analyzed by C. Dodd. R. K. Saiki provided plasmids and samples of genomic DNA obtained from cell lines. J. Korenberg and K. Tanaka made available blood samples from sickle cells patients. The *N*-hydroxysuccinimide ester of carboxy-2',7'-dimethoxy-4',5'-dichlorofluorescein was provided by M. W. Hunkapiller. We acknowledge discussions with B. Korber, B. Popko, A. Kamb, N. Lan, L. Smith, R. Barth, V. A. McKusick, J. Richards, and M. Simon.

11 April 1988; accepted 23 June 1988

Amyloid Protein Precursor Messenger RNAs: Differential Expression in Alzheimer's Disease

M. R. PALMERT, T. E. GOLDE, M. L. COHEN, D. M. KOVACS, R. E. TANZI, J. F. GUSELLA, M. F. USIAK, L. H. YOUNKIN, S. G. YOUNKIN*

In situ hybridization was used to assess total amyloid protein precursor (APP) messenger RNA and the subset of APP mRNA containing the Kunitz protease inhibitor (KPI) insert in 11 Alzheimer's disease (AD) and 7 control brains. In AD, a significant twofold increase was observed in total APP mRNA in nucleus basalis and locus ceruleus neurons but not in hippocampal subicular neurons, neurons of the basis pontis, or occipital cortical neurons. The increase in total APP mRNA in locus ceruleus and nucleus basalis neurons was due exclusively to an increase in APP mRNA lacking the KPI domain in nucleus basalis and locus ceruleus neurons may play an important role in the deposition of cerebral amyloid that occurs in AD.

ALZHEIMER'S DISEASE (AD) IS characterized pathologically by large numbers of senile plaques and neurofibrillary tangles throughout the cerebral cortex and hippocampus. Senile plaques consist of clusters of degenerating neurites surrounding an amyloid core composed of 5- to 10-nm fibrils that stain metachromatically with Congo red. In many cases of AD, amyloid fibrils are also found in vessel walls (1). A 4.2-kD polypeptide, referred to as A4 or the β protein, has been isolated from the amyloid fibrils found in senile plaques (2) and vessel walls (3) of patients with AD. There is evidence that A4 may also be a component of the paired helical filaments found in neurofibrillary tangles (4).

The gene encoding A4, which is located on chromosome 21 (5), produces at least three mRNAs (Fig. 1) referred to as APP₆₉₅, APP₇₅₁, and APP₇₇₀ (6-8). APP₆₉₅, the mRNA that was initially identified (5), en-

codes an amyloid protein precursor (APP), 695 amino acids in length, that includes A4 at positions 597 to 638. APP₇₅₁ is identical to APP₆₉₅, except for a 168-nucleotide insert (6-8). This insert, previously referred to as HL124i (7), would introduce 56 amino acids carboxyl terminal to Arg²⁸⁸ and convert Val²⁸⁹ into an isoleucine. APP₇₇₀ is identical to APP₇₅₁, except for a 57-nucleo-

M. R. Palmert, T. E. Golde, M. F. Usiak, L. H. Younkin, S. G. Younkin, Division of Neuropathology, Institute of Pathology and Department of Pharmacology, Case Western Reserve University School of Medicine, Cleveland, OH 44106.

M. L. Cohen and D. M. Kovacs, Division of Neuropathology, Institute of Pathology, Case Western Reserve University School of Medicine, Cleveland, OH 44106. R. E. Tanzi and J. F. Gusella, Neurogenetics Laboratory, Massachusetts General Hospital and Department of Genetics and the Program in Neuroscience, Harvard Medical School, Boston, MA 02115.

*To whom correspondence should be addressed at the Department of Pharmacology.

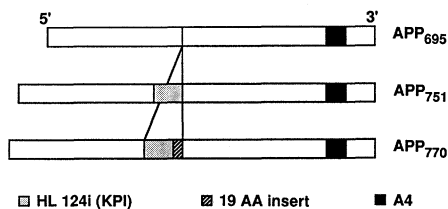


Fig. 1. Schematic illustration of the relative size and position of the A4 domain and the domains encoded by the alternatively spliced exons in the APP gene.

tide insert (8). This insert would introduce 19 amino acids COOH-terminal to the domain encoded by HL124i and convert Val²⁸⁹ into a leucine. In genomic DNA, the 168- and 57-nucleotide RNA inserts are encoded in two exons separated by an intron of about 3 kb and flanked by intron-exon consensus sequences (8). Thus the three mRNA species appear to arise through alternative splicing of two exons in the single-copy APP gene. The three APP mRNAs appear to be differentially regulated because RNA gel blot analyses indicate that their relative amounts differ in various cultured cells and in various fetal and adult tissues (6–8).

The sequence of the 56-amino acid insert encoded by HL124i is highly homologous to Kunitz-type protease inhibitors (6–8), which are specific for serine proteases such as trypsin, chymotrypsin, elastase, plasmin, and cathepsin G (9). Moreover, there is evidence that this insert confers trypsin-inhibitory activity upon transfected COS-1 cells (8). Although this domain could serve a variety of functions relevant to AD (10), its potential role in amyloidogenesis is particularly intriguing. If this domain functions as a protease inhibitor *in vivo*, it could, depending on its specificity, either promote amyloidogenesis (by inhibiting proteases that degrade A4) or impede amyloidogenesis (by inhibiting proteases involved in the generation of A4 from the APP).

In this study we used *in situ* hybridization to assess APP mRNA in several different neuronal populations of 11 sporadic AD (11) and 7 control brains well matched for age (AD, 75.6 ± 2.1 years; control, 73.7 ± 2.8 years) and postmortem interval (AD, 4.2 ± 0.4 hours; control, 4.7 ± 0.9 hours). Total APP mRNA and the subset of APP mRNA containing the Kunitz protease inhibitor (KPI) insert were assessed in separate experiments. To evaluate total APP mRNA, we hybridized with a ³⁵S-labeled RNA (cRNA) complementary to the 3' untranslated region found in all of the APP mRNAs [bases 2801 to 3143 of the APP₇₅₁ sequence published by Ponte *et al.* (6)]. To evaluate APP mRNA containing the KPI insert, we hybridized with a ³⁵S-labeled

cRNA complementary to HL124i [bases 1019 to 1138 of the Ponte sequence (6)]. In each experiment, sets of AD and control sections from the same brain region were processed side by side to optimize comparison of mRNA levels in AD and control cases. Antisense cRNA was applied to three serial cryostat sections from each tissue block, and, to control for nonspecific binding, a fourth serial section was hybridized with noncomplementary RNA of the same size, concentration, and specific activity [additional methodological details can be found in (11)].

In every experiment the antisense probes for total APP and KPI insert-containing mRNA labeled neuronal perikarya in the AD and control cases, whereas the noncomplementary probes produced very few grains above the emulsion background (Figs. 2 to 4). We did not observe specific grains (grains with antisense probe minus grains with sense probe) over glial or endothelial cells in either AD or control cases.

The results of our quantitative analysis of APP mRNA in various brain regions are summarized in Fig. 5. In our initial experiments, we focused on the nucleus basalis of Meynert (nbM) and the locus ceruleus (LC), two subcortical nuclei that project diffusely to the cerebral cortex, degenerate in AD (12, 13), and have axons that are found in senile plaques (14). In the nbM, the probe for total APP mRNA (Fig. 2, A and B) produced 95% more specific grains over cholinergic neurons in the 11 AD cases (80 ± 6) than in the 7 controls (41 ± 10) ($P = 0.005$). The probe for KPI-containing APP mRNA (Fig. 3, A and B), however,

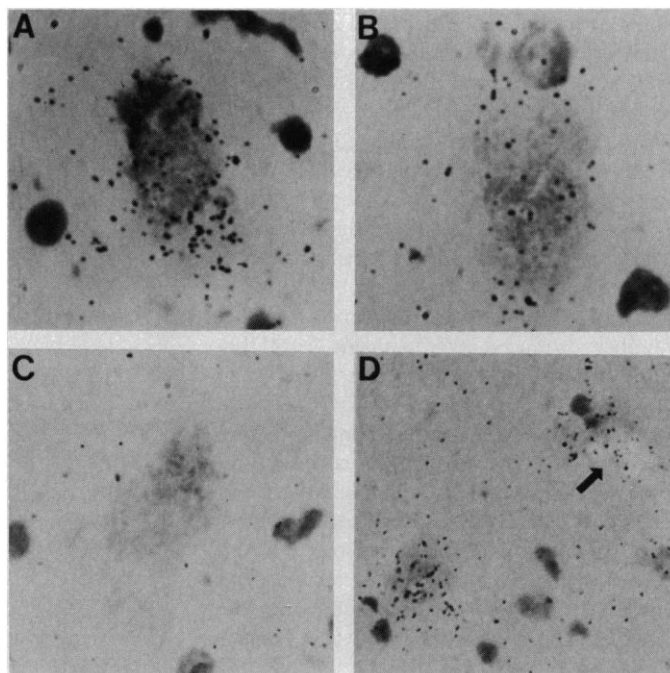
produced essentially the same number of specific grains in these same AD (57 ± 7) and control (60 ± 11) cases. Thus the expression of the APP gene is significantly increased in AD nucleus basalis neurons, and this increase appears to be due exclusively to an increase in APP mRNA lacking the protease inhibitor domain. The fact that only this form (presumably all APP₆₉₅) increases is interesting because it indicates that there is altered post-transcriptional processing of APP mRNA in AD.

In the LC (Figs. 4 and 5), the probe for total APP mRNA produced 94% more specific grains over pigmented noradrenergic neurons in the AD cases (180 ± 19) than in the controls (93 ± 18) ($P = 0.02$). As in the nbM, the probe for KPI-containing APP mRNA produced the same number of specific grains in the AD (63 ± 6) and control (62 ± 10) cases. Thus LC neurons also showed a significant increase in APP mRNA in AD, and, as in the nbM, the increase was due exclusively to an increase in APP mRNA lacking the KPI domain.

To evaluate APP mRNA in LC and nbM neurons undergoing neurofibrillary degeneration, we analyzed APP mRNA in neurofibrillary tangle-bearing and tangle-free neurons after staining with Congo red. The probes for both total and KPI-containing mRNA consistently produced fewer specific grains over the tangle-bearing than over the tangle-free neurons. Thus the increases in APP mRNA that we observed were largely due to changes in tangle-free rather than tangle-bearing neurons.

Analysis of subicular hippocampal neurons, another population that shows marked

Fig. 2. *In situ* hybridization with a ³⁵S-labeled cRNA probe for total APP mRNA. (A) AD nbM. (B) Control nbM. (C) Control nbM, noncomplementary probe matched to the probe for total APP mRNA. (D) AD subiculum. The closed arrow identifies a neurofibrillary tangle within a subicular neuron. Hybridizations were performed with 0.6 nM probe (3×10^9 cpm/nmol), and the autoradiographic exposure time was 1 day. Stain: (A to C) 0.4% cresyl violet in water; (D) hematoxylin and Congo red. Methodological details are in (11). Magnification: (A to C) $\times 1250$; (D) $\times 900$.



degenerative changes in AD, gave results very different from those observed in nbM and LC neurons. In the 11 AD and 7 control cases, the number of specific grains produced over subicular neurons by the probe for total APP mRNA (AD, 43 ± 5 ; control, 48 ± 6) and the probe for KPI insert-containing mRNA (AD, 37 ± 5 ; control, 38 ± 3) was essentially identical in the AD and control cases (Fig. 5). In an effort to identify changes that might have been missed in analyzing the subicular population as a whole, we evaluated tangle-bearing and tangle-free neurons separately in Congo red-stained sections from 5 of the AD cases. With the probe for total APP mRNA (Fig. 2D) and the probe for KPI-containing APP mRNA (Fig. 3D), the number of specific grains produced over tangle-bearing neurons was essentially the same as that over tangle-free neurons. Thus subicular neurons differ from those in the nbM and LC in that the pathologic process that occurs in subicular neurons is not associated with an increase in APP mRNA. Higgins *et al.* evaluated total APP mRNA in the hippocampus and reported increased APP gene expression in parasubicular neurons in AD (15), but Higgins (16) has also found no change in neurons of the subiculum.

In five of the AD and control cases, the same sections used to evaluate LC neurons were also used to evaluate grains over neurons in the basis pontis, a population that does not appear to be affected by AD. The specific grains produced over these neurons by the probe for total APP mRNA (AD, 45 ± 6 ; control, 35 ± 8) and the probe for KPI insert-containing mRNA (AD, 33 ± 4 ; control, 25 ± 4) were not significantly different in the AD and control cases.

In a preliminary assessment of cerebral cortex, we analyzed the occipital region where neurons in the vicinity of amyloid plaque cores could be evaluated easily. In sections stained with Congo red, we analyzed occipital cortical neurons adjacent to amyloid plaque cores in five of the AD cases. The number of specific grains produced over these neurons by the probe for total APP mRNA was essentially identical to the number produced over neurons from the same region in five control cases. The same result was obtained after hybridization with the probe for APP mRNA containing the KPI insert. Thus, in cerebral cortex as in subiculum and basis pontis, we have been unable to demonstrate altered expression of the APP gene in AD. Additional data on other cerebral cortical regions are needed, however, before concluding that APP gene expression in the cerebral cortex is not affected by AD.

The fact that increases in APP mRNA lacking the KPI domain occur in nbM and LC neurons but not in others could be due to a selective effect of AD pathology on

neurons, such as those in the nbM and LC, that have long, arborizing axons that project diffusely to cerebral cortex. An alternative possibility, consistent with our observation

Fig. 3. In situ hybridization with a ^{35}S -labeled cRNA probe for APP mRNA containing the KPI insert. (A) AD nbM. (B) Control nbM. (C) Control nbM, non-complementary probe matched to the probe for KPI-containing APP mRNA. (D) AD subiculum. Closed arrows identify neurofibrillary tangles within subicular neurons. Open arrows identify ghost tangles. Notice that there are no grains over the ghost tangles. Hybridizations were performed with 0.6 nM probe (1×10^9 cpm/nmol), and the autoradiographic exposure time was 4 days. Stain: (A to C) 0.4% cresyl violet in water; (D) hematoxylin and Congo red. Methodological details are in (11). Magnification: (A to C) $\times 500$; (D) $\times 900$.

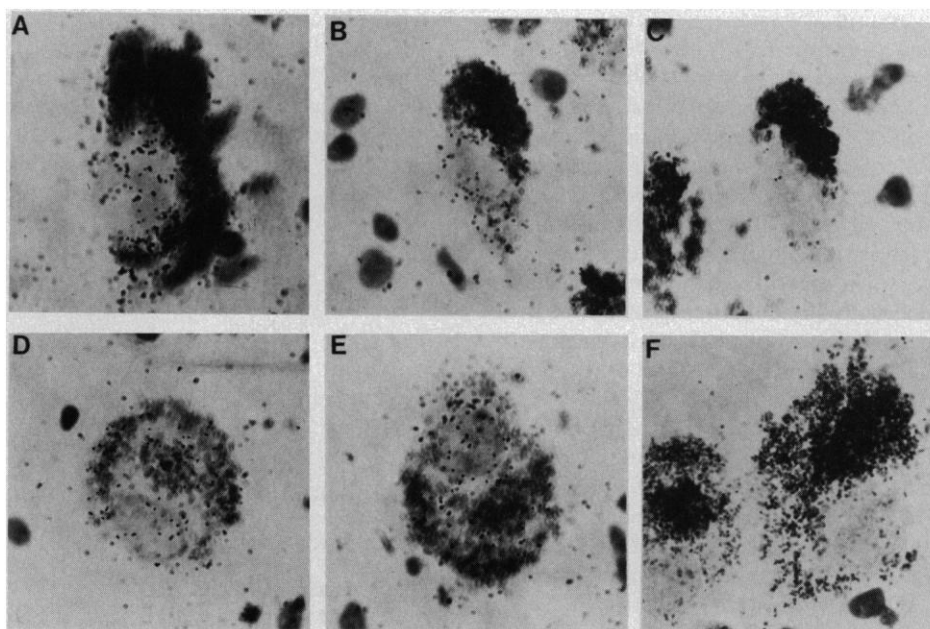
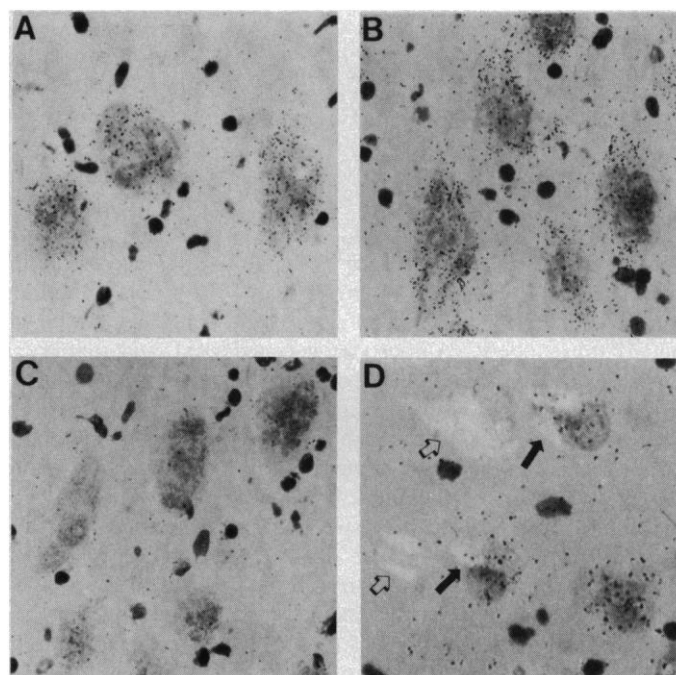


Fig. 4. In situ hybridization of LC neurons with ^{35}S -labeled cRNA probes. (A) AD, probe for total APP mRNA. (B) Control, probe for total APP mRNA. (C) Control, noncomplementary probe matched to the probe for total APP mRNA. (D) AD, probe for KPI-containing APP mRNA. (E) Control, probe for KPI-containing APP mRNA. (F) Control, noncomplementary probe matched to the probe for KPI-containing APP mRNA. Although difficult to illustrate photographically, we readily distinguished exposed silver grains from the neuromelanin pigment in LC neurons by first focusing in the plane of the tissue section, to identify the perikaryon to be counted, and then focusing above the tissue section in the plane of the autoradiographic emulsion to count grains. Hybridizations for total APP mRNA were performed with 0.6 nM probe (3×10^9 cpm/nmol), and the autoradiographic exposure time was 1 day. Hybridizations for KPI-containing mRNA were performed with 0.6 nM probe (1×10^9 cpm/nmol), and the autoradiographic exposure time was 4 days. Stain, 0.4% cresyl violet in water. Methodological details are in (11). Magnification, $\times 1250$.

that increased expression occurs predominantly in tangle-free LC and nbM neurons, is that increased APP gene expression may occur as part of a compensatory response that develops uniquely in surviving nbM and LC neurons as other cells in these populations are lost.

Previous *in situ* hybridization studies by this (17) and other laboratories (18) have established that most, if not all, of the APP mRNA in the central nervous system (CNS) is produced by neurons. In their recent analysis of total APP mRNA in cerebral cortex, Lewis *et al.* (19) found no correlation between the density of positively hybridizing neurons in various regions of cerebral cortex and the density of Thioflavin S-stained neuritic plaques in those regions. On this basis, these authors suggested that the amyloid β protein in senile plaques might be derived from nonneuronal sources such as plasma proteins, from long corticocortical projection neurons, or from cortically projecting brainstem neurons.

In a previous study (17) using a ^{125}I -labeled oligonucleotide probe for total APP mRNA, we showed that cholinergic nbM neurons in patients with AD have significantly more total APP mRNA than controls. The present study with ^{35}S -labeled cRNA probes confirms this result, extends it to include LC neurons, and shows that increased APP gene expression does not occur in neurons of the subiculum, basis pontis, or cerebral cortex. Moreover, this study indicates that there is altered post-transcriptional processing of APP mRNA in AD because the increases that we observed occurred

exclusively in APP mRNA lacking the KPI domain. Our finding of increased APP mRNA lacking the KPI domain in AD correlates well with the observation that increased levels of amyloidogenic proteins frequently occur in the systemic amyloidoses (20) and suggests that the cerebral amyloid deposited in AD may derive largely from axons projected by nbM and LC neurons. Further studies will be required to determine if changes in post-translational processing also contribute to amyloid deposition in AD.

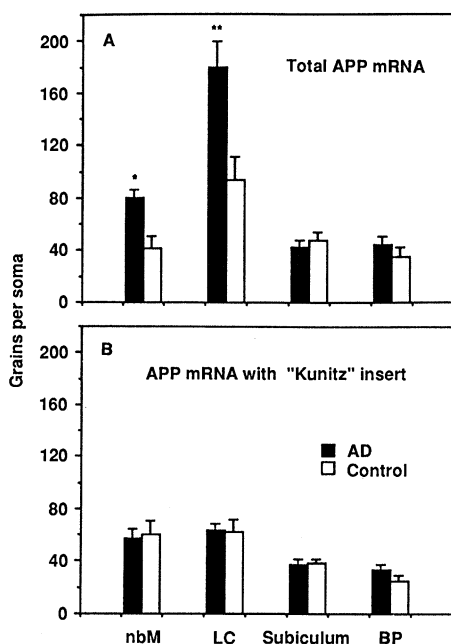
The position of the nucleotide sequence encoding A4 within the APP cDNAs that have been sequenced indicates that amyloid deposition requires the proteolytic cleavage of A4 from APP. If the KPI domain normally inhibits proteases that cleave A4 from the APP, then increased levels of amyloid protein precursor lacking this domain would accelerate the rate at which A4 is generated. Castano *et al.* (21) have shown that synthetic peptides corresponding to residues 1 to 28 and 17 to 28 of the 42-amino acid A4 polypeptide can form Congo red-positive amyloid fibrils *in vitro* under physiological conditions. Thus a sufficient amount of A4 may be all that is necessary to produce amyloid fibrils *in vivo*. We assume that the nbM and LC neurons with increased levels of KPI-free APP mRNA produce increased levels of the corresponding protein and transport it along their axons into the cerebral cortex. As a provisional working hypothesis, we propose that this KPI-free APP may be a substrate that is acted upon preferentially by cerebral proteases to generate

much of the A4 that is deposited as cerebral amyloid in AD (22).

REFERENCES AND NOTES

1. R. D. Terry *et al.*, *Ann. Neurol.* **10**, 184 (1981); G. G. Glenner, in *Banbury Report 15: Biological Aspects of Alzheimer's Disease*, R. Katzman, Ed. (Cold Spring Harbor Laboratory, Cold Spring Harbor, NY, 1983), pp. 137-144.
2. C. L. Masters *et al.*, *Proc. Natl. Acad. Sci. U.S.A.* **82**, 4245 (1986).
3. G. G. Glenner and W. C. Wong, *Biochem. Biophys. Res. Commun.* **122**, 1131 (1984).
4. C. L. Masters *et al.*, *EMBO J* **4**, 2757 (1985); D. C. Guioy *et al.*, *Proc. Natl. Acad. Sci. U.S.A.* **84**, 2073 (1987).
5. D. Goldgaber, M. I. Lerman, O. W. McBride, U. Saffiotti, D. C. Gajdusek, *Science* **235**, 877 (1987); J. Kang *et al.*, *Nature* **325**, 733 (1987); R. E. Tanzi *et al.*, *Science* **235**, 880 (1987); N. K. Robakis *et al.*, *Lancet* **i**, 384 (1987).
6. P. Ponte *et al.*, *Nature* **331**, 525 (1988).
7. R. E. Tanzi *et al.*, *ibid.*, p. 528.
8. N. Kitaguchi, Y. Takahashi, Y. Tokushima, S. Shiojiri, H. Ito, *ibid.*, p. 530.
9. G. J. Albrecht, K. Hochstrasser, J. P. Salier, *Hoppe Seyler's Z. Physiol. Chem.* **364**, 1703 (1983); B. J. Bromke and F. Kueppes, *Biochem. Med.* **27**, 56 (1982).
10. R. W. Carrell, *Nature* **331**, 478 (1988).
11. All 11 of the AD cases evaluated had neuritic plaques throughout the cerebral cortex in numbers well above those required for a diagnosis of AD (23), showed classic hippocampal pathology, and showed the expected reduction in cholinergic nbM (12) neurons and LC (13) neurons. The neuronal decrease in our AD cases ranged from 26 to 89% of the mean control value in the nbM (mean decrease = 69%, $P < 0.001$, Student *t* test) and from 31 to 92% in the LC (mean decrease = 72%, $P = 0.013$ by Student *t* test). We analyzed cholinergic nbM neurons [neurons with diameters of over 20 μm that were clustered between the lateral anterior commissure and medial optic tract (24)]; LC neurons (large pigmented neurons clustered appropriately in the floor of the lateral fourth ventricle); basis pontis neurons (neurons located in the midst of the bundles of myelinated fibers that traverse the basis pontis); hippocampal subicular neurons [the location of the subiculum is documented in figure 1 of Higgins *et al.* (15)]; and neurons of the occipital cortex. The cRNA probes were transcribed conventionally using ^{35}S -labeled uridine triphosphate (UTP). The probe for total APP mRNA was complementary to bases 2801 to 3143 of the APP₇₅₁ sequence published by Ponte *et al.* (6). The probe for HL124i-containing APP mRNA was complementary to bases 1019 to 1138 of the Ponte sequence (6). RNA gel blot analysis of total RNA from adult rat brain, liver, and kidney, and human fibroblast cell lines using our probes for total and HL124i-containing APP mRNA showed single bands of about 3.2 to 3.4 kb similar to those published previously (5, 7). Tissue blocks were rapidly frozen by immersion in isopentane cooled with liquid nitrogen. Cryostat sections (12 μm) were air dried, fixed 5 min in 4% (wt/vol) paraformaldehyde in 0.1M sodium phosphate (pH 7), rinsed in 2 \times saline sodium citrate (SSC), treated 10 min with freshly prepared 0.25% acetic anhydride in 0.1M triethanolamine buffer (pH 8), rinsed in 2 \times SSC, dehydrated by passage through increasing ethanol concentrations (70%, 1 min; 80% 1 min; 95%, 2 min), and hybridized with 20 μl of hybridization solution at 58°C under baked glass cover slips covered with oil. The hybridization solution contained 0.5 mg of salmon sperm DNA per milliliter, 1 mg of *Escherichia coli* transfer RNA per milliliter, 300 mM dithiothreitol, 50% formamide, 1 mM EDTA, 20 mM tris-HCl (pH 8), 0.3M NaCl, 10% polyethylene glycol, 5 \times Denhardt's solution, and 0.6 nM probe. After hybridization, sections were dipped in chloroform to remove the oil, washed at 50°C for 5 min in 1 \times SSC containing 300 mM β -mercaptoethanol and for 20

Fig. 5. Specific grains localized over neuronal perikarya in various brain regions of AD and control cases. The 11 AD and 7 control cases analyzed were well matched for age (AD, 75.6 ± 2.1 ; control, 73.7 ± 2.8 years) and post-mortem interval (AD, 4.2 ± 0.4 ; control, 4.7 ± 0.9 hours). The grain counts shown are the mean \pm SEM and are expressed per average somal area as described in (11). Each bar shows the mean of 5 to 11 cases and represents composite data from counts of at least 600 perikarya in the nbM, 200 perikarya in the locus ceruleus (LC) (where AD cases often had few surviving neurons), 600 perikarya in the subiculum, and 450 perikarya in the basis pontis (BP) (A). Specific grains (grains with antisense probe minus grains with noncomplementary probe) produced by the probe for total APP mRNA. $*P = 0.005$; $**P = 0.02$ by Student *t* test. (B) Specific grains produced by the probe for KPI insert-containing APP mRNA. The amount of total and KPI-containing APP mRNA cannot be compared directly from the data shown because they were analyzed in separate experiments: sections hybridized with the probe for total APP mRNA (3×10^9 cpm/nmol, 0.6 nM) were exposed for 1 day; those hybridized with the probe for KPI-containing APP mRNA (1×10^9 cpm/nmol, 0.6 nM) were exposed 4 days. Methodological details are in (11).



min in 1× SSC at 50°C, treated with 500 µg of ribonuclease A per milliliter in 4× SSC at 37°C for 30 min, washed twice for 40 min and 5 min in 1× SSC at 50°C, rinsed twice for 5 min in 2× SSC at room temperature, and dipped five times in water. After drying, sections were dipped in Kodak NTB-2 emulsion, exposed for 1 (total APP mRNA probe) or 4 (HL124i-containing APP mRNA) days, developed for 2 min with Kodak D-19, and fixed in Kodak Rapid Fix for 1.5 min. After copious rinsing in distilled water, sections were stained with cresyl violet or hematoxylin and Congo red, dehydrated, and mounted. To quantitate the hybridization of the APP probes to mRNA within perikarya in the various brain regions examined, we focused on the plane of the cells, identified the perikaryon to be assessed at ×1000 magnification, and superimposed a grid of a size chosen so that it just fit within that perikaryon. We then adjusted the focus so that the grains within the grid (which are not clearly visible when one focuses on cells) could all be counted. In each tissue block, the average number of grains produced over perikarya by antisense probe was typically obtained by analyzing 30 randomly chosen neurons on each of two or three sections, and the number produced by noncomplementary probe was obtained by analyzing 30 randomly chosen neurons on one section. The number of grains produced by the specific binding of antisense probe was then calculated by taking the difference between the antisense and noncomplementary grain counts. The antisense/sense ratio ranged from 5:1 to 10:1 in the various cell types examined. To illustrate the relative amount of APP mRNA in some of the various regions that we examined, we have expressed specific grain counts per average somal area. Average somal sizes, which were not appreciably different in the AD and control cases, were determined by averaging morphometric measurements made on three AD and three control cases with the Bioquant II system (R&M Biometrics) (nbM 700, LC 809, basis pontis 264, and subiculum 262 µm²).

12. P. J. Whitehouse *et al.*, *Science* **215**, 1237 (1982).
13. B. Maryciuk, D. M. A. Mann, P. O. Yates, *J. Neurol. Sci.* **76**, 335 (1986).
14. C. A. Kitt *et al.*, *Neuroscience* **16**, 691 (1985); L. C. Walker *et al.*, *J. Neuropathol. Exp. Neurol.* **47**, 138 (1988); D. M. Armstrong, G. Bruce, L. B. Hersh, R. D. Terry, *Neurosci. Lett.* **71**, 229 (1986).
15. G. Higgins *et al.*, *Proc. Natl. Acad. Sci. U.S.A.* **85**, 1297 (1988).
16. G. Higgins, personal communication.
17. M. L. Cohen, T. E. Golde, M. F. Usiak, L. H. Younkin, S. G. Younkin, *Proc. Natl. Acad. Sci. U.S.A.* **85**, 1227 (1988).
18. S. Bahmanyar *et al.*, *Science* **237**, 77 (1987); M. Goedert, *EMBO J.* **6**, 3627 (1987).
19. D. A. Lewis *et al.*, *Proc. Natl. Acad. Sci. U.S.A.* **85**, 1691 (1988).
20. A. S. Cohen and L. H. Connors, *J. Pathol.* **151**, 1 (1987); E. M. Castano and B. Frangione, in *Alterations in the Neuronal Cytoskeleton in Alzheimer Disease*, G. Perry, Ed. (Plenum, New York, 1987), pp. 33–44; R. Kisilevsky, *Can. J. Physiol. Pharmacol.* **65**, 1805 (1988).
21. E. M. Castano *et al.*, *Biochem. Biophys. Res. Commun.* **141**, 782 (1986).
22. The increased KPI-free APP mRNA observed in this study occurred in two nuclei in which there was a marked loss of neurons (11). This neuronal loss does not, however, obviate the potential significance of the increased KPI-free APP mRNA that we observed. The amount of amyloid deposited would, according to our working hypothesis, depend on (i) the duration of the increase in the affected neurons, (ii) the size of the neuronal population showing increased KPI-free APP, and (iii) the percentage increase in the KPI-free form in the affected neurons. We do not know when elevated levels of KPI-free APP mRNA develop during the protracted course of AD. The effect of elevated KPI-free APP mRNA will be greatest if this increase is an early, persistent change that develops prior to the loss of nbM or LC neurons and least if it is a brief end-stage phenomenon that occurs after the depletion of the nbM and LC populations. We have no direct evidence regarding the duration of the change in APP

gene expression, but there was no statistically significant correlation between the degree of cell loss in the nbM or LC and the increase in total APP mRNA. Neurons tended, if anything, to show progressively greater increases in total APP mRNA as the number of surviving neurons increased, and cases with many surviving neurons showed marked increases in total APP mRNA. In the AD case with the least loss of nbM neurons (26%), for example, the probe for total APP mRNA produced 2.8 times more specific grains over nbM perikarya than in the mean control case. It should also be emphasized that it is the change in KPI-free APP mRNA rather than the increase in total APP mRNA that is important for amyloid deposition according to our hypothesis. Although we did not directly evaluate KPI-free APP mRNA in this study, analysis of our data suggests that this form is a small fraction of total APP mRNA in control nbM and LC neurons. Thus, in AD, the twofold increase in total APP mRNA (which occurred exclusively in APP mRNA lacking the KPI

domain) appears to occur because of a dramatic percentage increase in the relevant KPI-free transcript.

23. Z. S. Khachaturian, *Arch. Neurol.* **42**, 1097 (1985).
24. P. L. McGeer *et al.*, *Neurology* **34**, 741 (1984).
25. We thank the morticians at University Hospitals in Cleveland (E. Kubu, R. Schnierer, S. Shopp, J. Skrel, F. Sabo, J. Verdone, and J. Wenzel) for their support in our acquisition of the tissue used in this study; A. Vitale for cutting the cryostat sections; C. Berman for staining sections with Congo red; R. Repasky for counting the nucleus basalis neurons; and L. Gambetti, P. Gambetti, S. Landis, J. Nilson, G. Perry, T. Rosenberry, R. Siegel, and P. Whitehouse for reviewing the manuscript. We thank B. Muller-Hill for providing the 1-kb APP Eco RI restriction fragment. Supported by USPHS grants AG06656, MH43444, and 5T32GM07250 and a grant from the State of Ohio.

30 March 1988; accepted 23 June 1988

Conferring Operator Specificity on Restriction Endonucleases

MICHAEL KOOB, ERIC GRIMES, WACLAW SZYBALSKI*

Mapping and manipulation of very large genomes, including the human genome, would be facilitated by the availability of a DNA cleavage method with very high site specificity. Therefore, a general method was devised that extends the effective recognition sequences well beyond the present 8–base pair limit by combining the specificity of the restriction endonuclease with that of another sequence-specific protein that binds tightly to DNA. It was shown that the tightly binding *lac* or λ repressor protects a restriction site within the operator from specific modification methylases, M·Hha I or M·Hph I, while all other similar sites are methylated and thus rendered uncuttable. A plasmid containing a symmetric *lac* operator was specifically cleaved by Hha I, only at the site within the operator, after M·Hha I methylation in the presence of the *lac* repressor, whereas the remaining 31 Hha I sites on this plasmid were methylated and thus not cleaved. Analogous results were obtained with the Hae II site within the *lac* operator, which was similarly protected by the *lac* repressor, and with the Hph I site within the phage λ σ_L operator, which was protected by λ repressor from M·Hph I methylation.

THE PRESENTLY AVAILABLE RESTRICTION enzymes cleave DNA at recognition sites of 4 to 8 bp. Statistically, 8-bp recognition leads to one cut per 65.5 kb. For mapping, manipulation, and sequencing of very large genomes (1) restriction systems with higher specificity are required. One of these systems is based on the natural methylation of many genomes, but such an adventitious modification process is not easy to control. Another, which has been shown to stretch effective recognition sites to 10 bp, is based on the joint use of modification methylases and restriction endonucleases for a few specific combinations of restriction sites (2–4). Finally, a number of laboratories have recently sought to create synthetic DNA-cleaving reagents by combining a sequence-specific DNA-bind-

ing domain with a DNA-cleaving moiety (5–7). However, the practical applications of these reagents are severely limited by their very low cleavage efficiency and inability to generate well-defined ends.

We have devised a general method (Fig. 1A) for efficiently extending the effective recognition sequence of a restriction endonuclease well beyond previous limits. Our method combined the activities of three proteins: (i) a repressor, which specifically binds to only very rare sites (operators) of about 20 bp in length; (ii) a modification methylase, which methylates all corresponding restriction sites with the exception of those protected by the repressor; and (iii) a restriction endonuclease with the same specificity as the modification methylase (Fig. 1A). The two specific examples we describe are operator-repressor systems of (i) the *lac* operon, which creates an effective recognition sequence of 20 bp, and (ii) the phage λ σ_L operator, which gives an effective

McArdle Laboratory for Cancer Research, University of Wisconsin, Madison, WI 53706.

*To whom correspondence should be addressed.